

Hypercrosslinked poly(styrene-co-divinylbenzene) resin as a specific polymeric adsorbent for purification of berberine hydrochloride from aqueous solutions

Yin Li ^{a,b}, Ruofan Cao ^b, Xiaofei Wu ^b, Jianhan Huang ^{b,c,d,*}, Shuguang Deng ^{a,b,*}, Xiuyang Lu ^{a,*}

^a Key Laboratory of Biomass Chemical Engineering of Ministry of Education, Department of Chemical and Biological Engineering, Zhejiang University, Hangzhou 310027, China

^b Chemical Engineering Department, New Mexico State University, Las Cruces, NM 88003, USA

^c School of Chemistry and Chemical Engineering, Central South University, Changsha 410083, China

^d Key Laboratory of Resources Chemistry of Nonferrous Metals of Ministry of Education, Changsha 410083, China

ARTICLE INFO

Article history:

Received 3 January 2013

Accepted 9 March 2013

Available online 21 March 2013

Keywords:

Hypercrosslinked

Resin

Adsorption

Purification

Berberine hydrochloride

Molecular sieving

ABSTRACT

A hypercrosslinked poly(styrene-co-divinylbenzene) resin (TEPA) was synthesized and characterized as a specific polymeric adsorbent for concentrating berberine hydrochloride from aqueous solutions. Three organic molecules of different sizes (2-naphthol, berberine hydrochloride, and Congo red) were used as target molecules to elucidate the molecular sieving effect of the TEPA adsorbent. Because the TEPA adsorbent has a pore structure consisting mainly of micropores and mesopores, the adsorption of 2-naphthol from aqueous solutions is very efficient due to the micropore filling effect. The adsorption of berberine hydrochloride mostly takes place in the mesopores as well as macropores, while the adsorption of Congo red mainly occurs in the macropores. The smaller adsorbate molecule (2-naphthol) reaches the adsorption equilibrium much faster than the larger ones (berberine hydrochloride and Congo red). An adsorption breakthrough experiment with an aqueous solution containing 2-naphthol and berberine hydrochloride demonstrated that the TEPA adsorbent could effectively remove 2-naphthol from berberine hydrochloride at 0–107 BV (bed volume, 1 BV = 10 ml), and the berberine hydrochloride concentration was increased from 66.7% to 99.4%, suggesting that this polymeric adsorbent is promising for purifying berberine hydrochloride and similar alkaloids from herbal plant extracts.

© 2013 Elsevier Inc. All rights reserved.

1. Introduction

Berberine hydrochloride is an isoquinoline derivative alkaloid that widely exists in the herbal plants. Berberine hydrochloride has many pharmacological effects such as anticancer activity, antibiotic property, and anti-inflammatory effect; it is being used as a natural medicine in several clinical applications [1,2]. Extraction of berberine hydrochloride from herbal plants is the most commonly approach to produce berberine hydrochloride. A series of time-consuming steps such as dissolving, filtration, recrystallization, and column separation are needed to obtain berberine hydrochloride with a relatively high purity. However, this approach is cumbersome and very difficult to achieve the required high purity because a large number of impurities are found in the herbal plant extracts. These impurities include many small water-soluble molecules such as phenol, 2-naphthol, and ferulic acid, which are very difficult to remove from raw materials by the conventional ap-

proaches [1]. As a result, selective separation and purification of berberine hydrochloride from herbal plant extracts are a very challenging task.

Adsorption is believed to be the most widely used and the most effective process for separation and purification of natural products like berberine hydrochloride. Silica gel (SiO₂), alumina (Al₂O₃), activated carbon, and polymer resins are the commonly used adsorbents for purification of natural products using the column chromatography [3]. However, efficient regeneration and high selectivity of the adsorbents are the two main problems. There are two ways to achieve the purification of certain compounds by adsorption. One approach is to adsorb the target compound by ion-exchange, hydrophobicity interaction, and hydrogen bonding, etc., and to recover the target compound in the desorption effluent. This technique has been extensively applied for the purification of natural products including berberine hydrochloride [3–5]. The other method is adsorbing or removing the coexisting impurities from the mixture and recovering the target molecules in the adsorption effluent [6]. However, no literature is currently available for concentrating berberine hydrochloride from aqueous solutions by the second approach.

Because of its unique pore structure and surface functionalities, hypercrosslinked poly(polystyrene-co-divinylbenzene) (PS) resin

* Corresponding authors. Address: Chemical Engineering Department, New Mexico State University, Las Cruces, NM 88003, USA (J. Huang, S. Deng). Fax: +86 731 88879616 (J. Huang), +86 571 87952683 (X. Lu), +1 575 646 7706 (S. Deng).

E-mail addresses: jianhanhuang@csu.edu.cn (J. Huang), sdeng@nmsu.edu (S. Deng), luxiyang@zju.edu.cn (X. Lu).

is widely used for adsorptive removal of aromatic compounds such as benzene, toluene, 2-naphthol, and phenol from aqueous solutions [7–9]. Besides the high adsorption capacity for aromatic compounds, this kind of polymeric adsorbent can be reused for more than 50 cycles and is being considered as a potential replacement of activated carbon for removal of organic compounds from wastewater [10–13]. Additionally, this type of resin has also been used as column packing materials in high-performance liquid chromatography (HPLC), ion size-exclusion chromatography materials and solid-phase extraction materials for gases, organic contaminants, and organic vapors [11,14–16]. Hypercrosslinked PS resin is generally synthesized from a linear PS or a low crosslinked PS by adding bifunctional crosslinking reagents and Friedel–Crafts catalysts [12,17], and it can also be prepared from a macroporous low crosslinked chloromethylated PS via its self Friedel–Crafts reaction [18]. By using this method, a large number of rigid crosslinked bridges are formed between the polymeric chains, which lead to a major shift of the pore diameter distribution of the hypercrosslinked resin from predominately mesopores to mesopores/micropores bimodal distribution, and a sharp increase in the Brunauer–Emmett–Teller (BET) surface area and pore volume [11,19]. Because of these significant changes, the hypercrosslinked PS resin exhibits excellent adsorption capacities for nonpolar and weakly polar aromatic compounds in aqueous solutions [20]. These resins are often modified by using polar compounds as the crosslinking reagent and addition of polar compounds to introduce polar units into the copolymers in the Friedel–Crafts reaction in order to increase their adsorption capacities toward polar aromatic compounds [21,22], and the modified hypercrosslinked resins exhibit improved adsorption properties toward polar aromatic compounds by introducing certain specific functional groups on the surface [12,23].

In this study, we aim at separating berberine hydrochloride from smaller molecules such as 2-naphthol from aqueous solutions by using a novel hypercrosslinked PS resin TEPA. For this purpose, the TEPA resin was synthesized, characterized, and evaluated for adsorption and separation of berberine hydrochloride from aqueous solutions. The molecular sieving effect of TEPA was illustrated by using three model molecules with different molecular size including 2-naphthol, berberine hydrochloride, and Congo red. The adsorption of these three adsorbates from aqueous solutions containing only single-component and solutions containing mixture of these adsorbates were performed and analyzed in detail. The separation capability of TEPA polymeric adsorbent was also demonstrated in an adsorption column breakthrough experiment with an aqueous solution containing a mixture of berberine hydrochloride and 2-naphthol.

2. Materials and methods

2.1. Materials

Macroporous crosslinked chloromethylated PS was purchased from Langfang Chemical Co. Ltd. (Hebei province, China), its crosslinking degree was 6%, its chlorine content was measured to be 17.3%, and its Brunauer–Emmett–Teller (BET) surface area and pore volume were determined to be 28 m²/g and 0.0036 cm³/g, respectively. 2-Naphthol, berberine hydrochloride, and Congo red applied as the adsorbates in this study were analytical reagents and purchased from Sigma–Aldrich, and they were used without any further purification. Their main properties including the molecular structure, molecular weight, and molecular size were listed in Table 1. The molecular size of these molecules was obtained from the optimized molecular structure performed by the Gaussian 09 software package. Density functional theory (DFT)

method with 6-31 G basis set was employed for the calculation, and the optimized molecular structure was achieved if there was no imaginary frequency. Their optimized molecular structure models obtained from the Gaussian 09 can be exhibited by the Gaussian View program and displayed in Fig. 1.

2.2. Synthesis of TEPA resin

For synthesis of TEPA resin, a typical hypercrosslinked PS polymeric adsorbent named HJ-11 was firstly prepared from macroporous crosslinked chloromethylated PS through a Friedel–Crafts alkylation reaction by using 1, 2-dichloroethane as the solvent and anhydride iron (III) chloride as the catalyst, and the synthesized procedure was performed according to the method in ref [13]. Thereafter, 20 g of HJ-11 was immersed in 100 ml of 1,2-dichloroethane at a room temperature overnight, superfluous 1,2-dichloroethane was then poured out, and 50 ml of tetraethylenepentamine was added into the reaction mixture. The reaction mixture was filtrated after keeping at 428 K for about 15 h, and the solid polymeric adsorbent TEPA was obtained. To remove the residual impurities in the pores of the solid particles, TEPA resin was firstly rinsed by a 1% of hydrochloric acid aqueous solution and followed by de-ionized water until neutral pH. After that, it was subjected to a 1% of sodium hydroxide aqueous solution and washed by de-ionized water until a neutral pH was obtained. Finally, the TEPA resins were extracted by anhydrous ethanol for 12 h and dried under a vacuum at 323 K for 8 h.

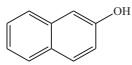
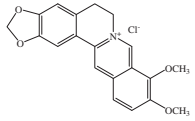
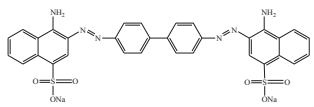
2.3. Characterization of the resins

The resins were characterized in terms of texture and chemical composition. For the textural characterization, the BET surface area, pore volume, and pore diameter distribution were determined by N₂ adsorption–desorption isotherms with the temperature at 77 K on a Micromeritics Surface Area and Porosimetry Analyzer ASAP 2020. Prior to the measurement, the samples were degassed under vacuum at 353 K for approximately 10 h. For the chemical composition characterization, the conventional chemical analysis of the resins such as the residual chlorine content, weak basic exchange capacity was determined according to the method in Refs. [24,25]. The Fourier-transformed infrared ray (FT-IR) spectra of the resins with vibrational frequencies in the range of 500–4000 cm⁻¹ were collected by KBr disks on a Spectrum 400 FT-IR spectrometer. The surface morphology, element composition, and particle size of the resin were carried out by scanning electron microscopy (SEM) equipped with energy dispersive X-ray spectroscopy (EDS). The concentration of 2-naphthol, berberine hydrochloride, and Congo red in aqueous solution was analyzed by Lambda 35 UV–VIS spectrometer at the wavelength of 274, 344, and 499 nm, respectively.

2.4. Adsorption equilibrium

About 0.1000 g of the resin was accurately weighed and introduced to a 50 ml of the adsorbate aqueous solution with known concentrations C₀ (mg/L) in a conical flask with a stopper (for the adsorption from the mixture solution, two series adsorbate solutions with known concentrations were simultaneously performed). The series of conical flasks were then shaken with a constant speed (200 rpm) for 6 h at 298 K in a thermostatic oscillator until the adsorption equilibrium was reached. The equilibrium concentration of the adsorbate C_e (mg/L) was analyzed, and the equilibrium adsorption capacity of the adsorbate on the resin q_e (mg/g) was calculated by conducting a mass balance on the adsorbate before and after the adsorption as:

Table 1
The main properties of 2-naphthol, berberine hydrochloride and Congo red.

Substance	Formula	Molecular Structure	Molecular weight	Molecular size
2-Naphthol	C ₁₀ H ₇ OH		144.2	0.80 nm × 0.53 nm
Berberine hydrochloride	C ₂₀ H ₁₈ ClNO ₄		371.8	1.47 nm × 0.66 nm × 0.32 nm
Congo red	C ₃₂ H ₂₂ N ₆ O ₆ S ₂ Na ₂		696.7	2.29 nm × 0.82 nm × 0.60 nm

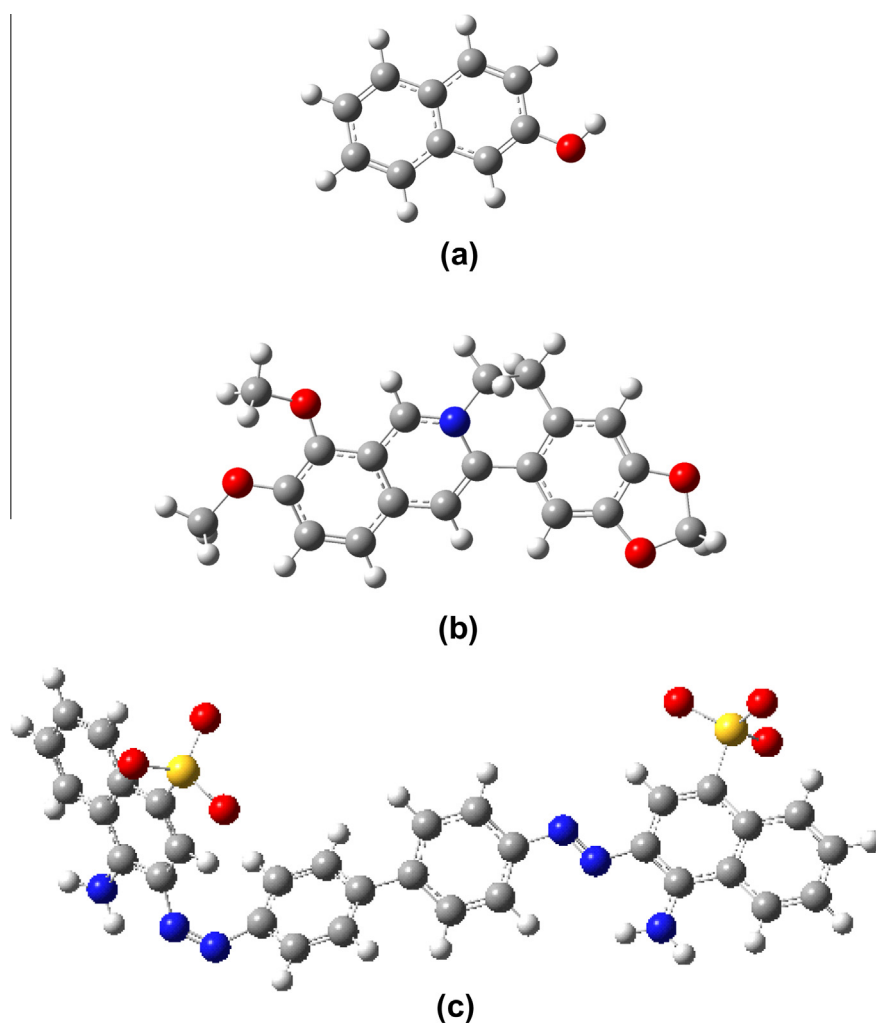


Fig. 1. Optimized molecular structure models of (a) 2-naphthol, (b) berberine hydrochloride, and (c) Congo red on Gaussian View program calculated by a Gaussian 09 software package.

$$q_e = (C_0 - C_e) \cdot V/W \quad (1)$$

where V is the volume of the solution (L) and W is the weight of the resin (g).

Competitive adsorption between 2-naphthol, berberine hydrochloride, and Congo red on the TEPA adsorbent was also investigated by measuring adsorption isotherms of these three adsorbate molecules using aqueous solutions containing mixture of these adsorbates. Experiments were also carried out by exposing

the TEPA adsorbent to one of the adsorbate molecules then measuring the adsorption isotherms of another adsorbate.

2.5. Adsorption kinetic

About 1.0000 g of the resin was firstly weighed and mixed with 250 mL of adsorbate aqueous solution in a 500 mL of the conical flask (an initial concentration of the adsorbate was set to be 400 mg/L). The flask was then continuously shaken in the

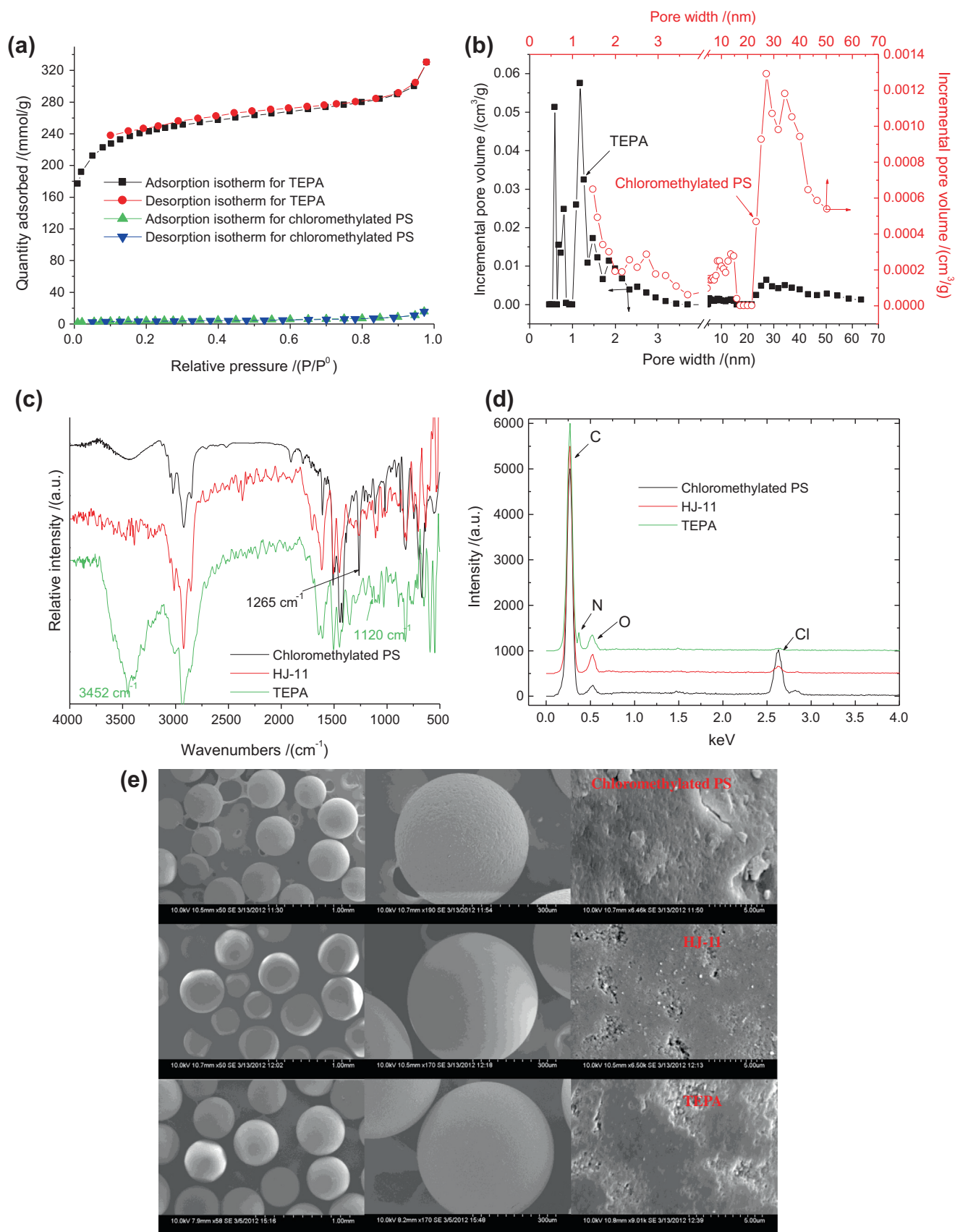


Fig. 2. Characterization results for the TEPA adsorbent: (a) N₂ adsorption-desorption isotherms; (b) pore diameter distribution (Density functional theory method, slit pore); (c) FT-IR spectra; (d) EDS; (e) SEM.

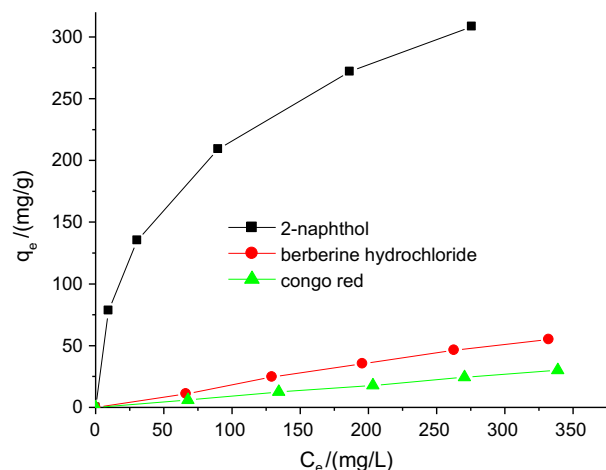


Fig. 3. Adsorption isotherms of 2-naphthol, berberine hydrochloride and Congo red on TEPA from single-component solutions at 298 K.

thermostatic oscillator at 298 K until the adsorption equilibrium was reached. During the shaking process, 0.5 mL of the adsorbate aqueous solution was withdrawn at a preset interval, the concentration of the adsorbate aqueous solution at the contact time t , C_t (mg/L), was recorded, and the adsorption capacity at the contact t , q_t (mg/g), was calculated as:

$$q_t = (C_0 - C_t) \cdot V/W \quad (2)$$

2.6. Dynamic adsorption and separation of berberine hydrochloride from a mixture solution

In the dynamic adsorption and separation experiment, 10 mL of wet TEPA resin was densely packed in a glass column with an inner diameter of 19 mm, and de-ionized water was continuously rinsed the resin column until the absorbance of the effluent from the resin column was zero. A synthetic mixture solution containing 1000 mg/L of berberine hydrochloride and 500 mg/L of 2-naphthol was passed through the resin column at a flow rate of 2.8 mL/min (16.8 BV/h, BV means bed volume, 1 BV = 10 mL). The effluents from the resin column were collected, and the concentration of berberine hydrochloride as well as 2-naphthol in the effluents was simultaneously monitored until it approached the initial one.

3. Results and discussion

3.1. Characterization of the resins

Fig. 2a compares the N_2 adsorption-desorption isotherms of TEPA with those of the chloromethylated PS. The N_2 adsorption capacity of TEPA is shown to be much larger than that of the chloromethylated PS at the same relative pressure, suggesting that the

BET surface area as well as the pore volume of TEPA is much higher than those of the chloromethylated PS. In fact, the BET specific surface area and pore volume of TEPA were measured to be 743.2 m^2/g and 0.5105 cm^3/g , respectively, much higher than those of the chloromethylated PS [26,27]. In addition, the micropore surface area and micropore volume of TEPA were determined to be 529.0 m^2/g and 0.2688 cm^3/g , respectively, which are more than one half of the total surface area and pore volume, implying that the micropores are the predominant pores in the TEPA adsorbent, which is consistent with the pore diameter distribution of TEPA plotted in Fig. 2b. Fig. 2b indicates that two typical pore regions are presented for TEPA, and the most predominant pores are the micropore (<2 nm), mesopores (2–50 nm), and macropores (>50 nm) also exist in this sample. In comparison, the structure of chloromethylated PS is dominated by macropores.

As displayed in Fig. 2c, the strong vibrational band related to C–Cl stretching of the CH_2Cl groups with frequency at 1265 cm^{-1} is greatly weakened after the Friedel–Crafts reaction, while all of the other vibrations remain the same, which indicates that the chlorine of the chloromethylated PS was consumed in the Friedel–Crafts reaction. This observation agrees with the results of the chlorine content of the resins. The residual chlorine content of HJ-11 was measured to be 3.20%, which is much lower than that of the chloromethylated PS (17.3%). Moreover, the results of EDS shown in Fig. 2d also support this result because the intensity of the chlorine of HJ-11 was much lower than that of the chloromethylated PS. Additionally, the residual chlorine content further reduced to 1.26%, and the weak basic exchange capacity for TEPA was measured to be 0.704 mmol/g of, implying that the residual chlorine on the surface of HJ-11 was further substituted by the amino groups (–NH– or –NH₂) of tetraethylenepentamine, and this deduction can also be confirmed by the vibrations at 3426 cm^{-1} (N–H stretching) and 1120 cm^{-1} (C–N stretching) in the FT-IR spectrum for TEPA. In particular, the result of EDS in Fig. 2d also supports this result because the intensity of the chlorine of TEPA was further reduced in comparison with HJ-11, while there appeared a new small peak related to the nitrogen atom in the EDS for TEPA. The SEM images of the chloromethylated PS, HJ-11, and TEPA are shown in Fig. 2e. It is interesting to see that the surface of HJ-11 is much smoother than that of the chloromethylated PS, while the surface of TEPA is rougher than that of HJ-11.

3.2. Adsorption isotherms of pure component

Fig. 3 displays the adsorption isotherms of 2-naphthol, berberine hydrochloride, and Congo red on TEPA. It seems that the adsorption of 2-naphthol on TEPA is very effective, and the equilibrium adsorption capacity of 210.0 mg/g was obtained at an equilibrium concentration of 100 mg/L at 298 K, which is much larger than that of other adsorbents such as commercial resins XAD-4 and XAD-7 as well as the hydroquinone modified hyper-crosslinked PS resin [22,28]. The relatively higher BET surface area and pore volume of TEPA (743.2 m^2/g and 0.5105 cm^3/g , respectively) are the primary reasons for the more efficient adsorption

Table 2
The fitted results for the adsorption of 2-naphthol, berberine hydrochloride, and Congo red on TEPA from the single solution according to Langmuir and Freundlich isotherm models with the temperature at 298 K.

	Langmuir model			Freundlich model		
	q_m (mg/g)	K_L (L/mg)	R^2	$K_F [(mg/g)(L/mg)^{1/n}]$	$1/n$	R^2
2-Naphthol	350.9	2.140×10^{-2}	0.9894	32.68	0.4053	0.9965
Berberine hydrochloride	1316	1.367×10^{-4}	0.05984	0.1780	0.9971	0.9917
Congo red	2326	3.896×10^{-5}	0.02492	9.119×10^{-2}	0.9973	0.9982

of 2-naphthol on TEPA. Meanwhile, the micropore surface area and micropore volume play dominant roles for TEPA, which are very suitable for the pore filling of 2-naphthol (molecular size: $0.80 \text{ nm} \times 0.53 \text{ nm}$) according to the micropore filling theory [29]. In particular, the surface of TEPA is modified by a few polar amino groups, which can be acted as the hydrogen bonding acceptor, and 2-naphthol is a polar molecule with a hydroxyl group, which can be employed as the hydrogen bonding donator, so the polarity matching (e.g., hydrogen bonding) can also enhance the adsorption affinity for 2-naphthol.

The adsorption capacity of 2-naphthol on TEPA is seen to be the largest, while that of Congo red is the smallest among the three adsorbates; only about 15% of berberine hydrochloride and 13% of Congo red were adsorbed on TEPA from aqueous solutions. The adsorption capacity of these three adsorbates on TEPA is in the order of $q_e(2\text{-naphthol}) \gg q_e(\text{berberine hydrochloride}) > q_e(\text{Congo red})$. The molecular sizes of 2-naphthol, berberine hydrochloride, and Congo red are predicted to be $0.80 \text{ nm} \times 0.53 \text{ nm}$, $1.47 \text{ nm} \times 0.66 \text{ nm} \times 0.32 \text{ nm}$, and $2.29 \text{ nm} \times 0.82 \text{ nm} \times 0.60 \text{ nm}$, respectively (Table 1), which follows the order of 2-naphthol < berberine hydrochloride < Congo red. TEPA shows the smallest adsorption capacity for the adsorbate with the largest molecular size (Congo red), while the adsorbate with a smallest molecular size (2-naphthol) has the largest adsorption capacity, suggesting a potential molecular sieving effect of the TEPA adsorbent for organic molecules of different sizes. According to the pore diameter distribution of TEPA (Fig. 2b), some mesopores (2–50 nm) as well as macropores (>50 nm) were found in the TEPA sample, which are responsible for the adsorption of berberine hydrochloride in the TEPA adsorbent. As for Congo red, only the macropores in the TEPA are accessible and useful for adsorbing Congo red, so its adsorption capacity is the smallest.

Langmuir and Freundlich isotherm models are applied to correlate the adsorption isotherm data, and the linear form of Langmuir and Freundlich isotherms is given as:

$$\text{Langmuir isotherm: } \frac{C_e}{q_e} = \frac{C_e}{q_m} + \frac{1}{K_L q_m} \quad (3)$$

$$\text{Freundlich isotherm: } \log q_e = \log K_F + \left(\frac{1}{n}\right) \cdot \log C_e \quad (4)$$

where q_m is the monolayer adsorption capacity (mg/g), K_L (mL/g) is the Langmuir constant, K_F and n are the Freundlich equation constants. K_F is an indicator of the equilibrium adsorption capacity, while n is related to the adsorption favorability or surface energy heterogeneity.

The model parameters such as q_m , K_L , K_F , and $1/n$ as well as the correlation coefficient R^2 for both Langmuir and Freundlich equations are summarized in Table 2. The larger correlation coefficient for the Freundlich equation suggests that the Freundlich isotherm model is more suitable for describing the adsorption isotherms presented in Fig. 3 [30].

When we compare the K_F for these three adsorbates, it is interesting to see that 2-naphthol (32.68) has a much larger K_F value than that of berberine hydrochloride (0.1780) and Congo red (9.119×10^{-2}), which is in consistent with equilibrium results of these three adsorbates on TEPA. Generally speaking, adsorption is easy to take place when $1/n$ value of the Freundlich equation is between 0.1 and 0.5, it is difficult to occur when $1/n$ value is between 0.5 and 1.0, and it is very difficult to occur when $1/n$ value exceeds 1 [31]. The $1/n$ values of 2-naphthol, berberine hydrochloride, and Congo red are calculated to be 0.4053, 0.9971, and 0.9973, respectively. Therefore, it is expected that the TEPA adsorbent can effectively remove 2-naphthol from berberine hydrochloride (or Congo red).

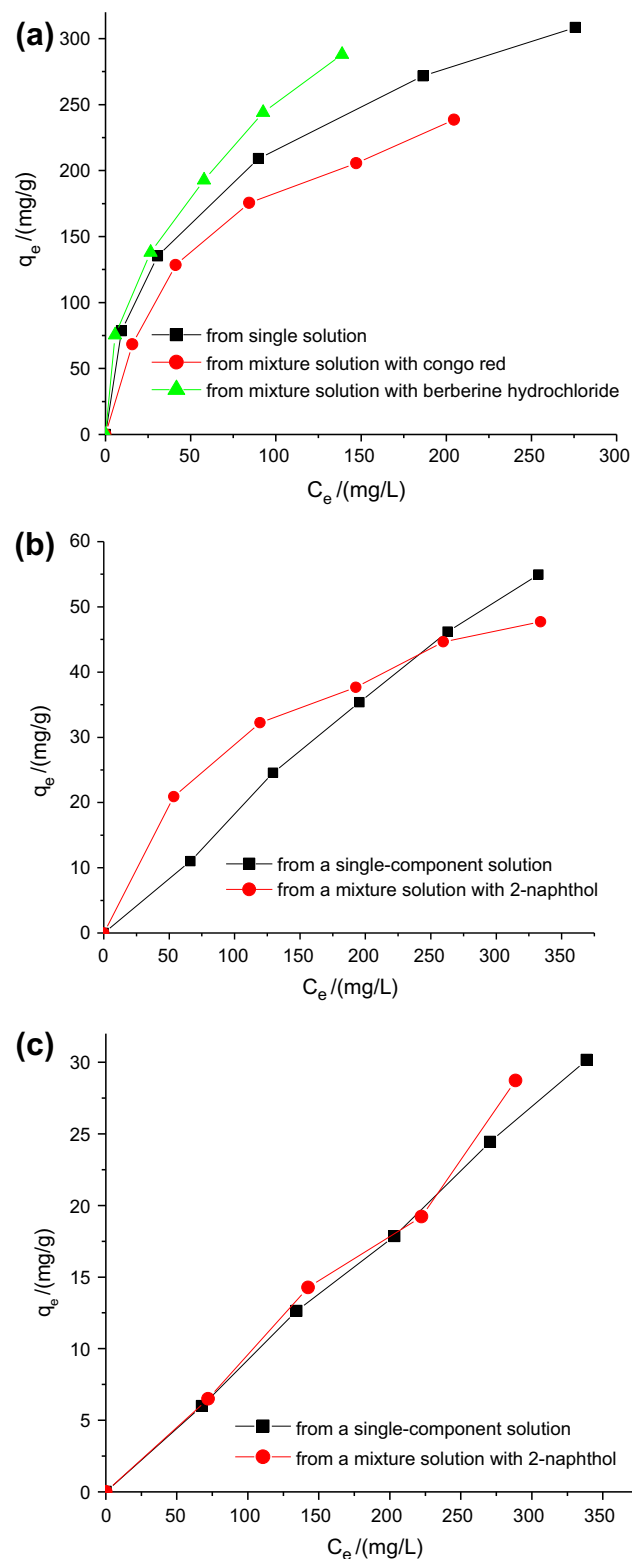


Fig. 4. Adsorption isotherms of (a) 2-naphthol, (b) berberine hydrochloride, (c) Congo red on TEPA resin from mixture solutions.

3.3. Competitive adsorption between 2-naphthol, berberine hydrochloride and Congo red

Fig. 4 compares the adsorption isotherms of three adsorbates obtained with single-component solutions and those with mixture solutions. Fig. 4a indicates that the effect of berberine

Table 3
The fitted results for the adsorption of 2-naphthol, berberine hydrochloride, and Congo red from the mixture solution according to Langmuir and Freundlich isotherm models.

	Langmuir isotherm model			Freundlich isotherm model		
	q_m (mg/g)	K_L (L/mg)	R^2	K_F [(mg/g)(L/mg) $^{1/n}$]	n	R^2
2-Naphthol						
Single adsorbate solution	350.9	2.140×10^{-2}	0.9894	32.68	2.467	0.9965
Mixture solution with berberine hydrochloride	340.1	3.033×10^{-2}	0.9649	35.79	2.381	0.9982
Mixture solution with Congo red	295.0	1.817×10^{-2}	0.9941	19.91	2.103	0.9757
Berberine hydrochloride						
Single adsorbate solution	1316	1.367×10^{-4}	0.05984	0.1780	1.003	0.9917
Mixture solution with 2-naphthol	63.86	8.528×10^{-3}	0.9924	3.519	2.206	0.9905
Congo red						
Single adsorbate solution	2326	3.896×10^{-5}	0.02492	9.119×10^{-2}	1.003	0.9982
Mixture solution with 2-naphthol	/	/	0.04953	8.109×10^{-2}	0.9719	0.9872

hydrochloride on the adsorption of 2-naphthol from a mixture solution is quite different from that of Congo red. When compared with adsorption isotherm obtained from single-component solutions, the adsorption of 2-naphthol from a mixture solution with Congo red is slightly weakened, while that from mixture solutions with berberine hydrochloride is slightly enhanced. The water solubility of berberine hydrochloride (0.1959 g/100 mL at 25 °C [32]) is much higher than that of 2-naphthol (0.0876 g/100 mL at 29.5 °C [33]). As berberine hydrochloride is added to the aqueous solution of 2-naphthol, a large number of water molecules are captured to dissolve berberine hydrochloride, which results in a “salt-out” effect for 2-naphthol [26], inducing an enhanced adsorption of 2-naphthol due to the higher hydrophobicity [34]. The molecular size of Congo red is so large that it blocks the diffusion of 2-naphthol from aqueous solution to the pores of TEPA as Congo red is coexistent with 2-naphthol, which leads to a weaker adsorption of 2-naphthol.

Fig. 4b displays that the adsorption isotherm of berberine hydrochloride from the mixture solution is different from the adsorption isotherm obtained from its single-component solution. Lower concentrations of 2-naphthol (<250 mg/L) have a positive effect on the adsorption of berberine hydrochloride, while higher concentrations (>250 mg/L) produce a negative effect. At lower concentrations of 2-naphthol, the adsorption sites of TEPA are more than the number of 2-naphthol molecules, and the pore structure of TEPA may be alerted to some degree after the adsorption of 2-naphthol, which may be more suitable for the adsorption of berberine hydrochloride. However, the strongly competitive adsorption of 2-naphthol on TEPA cannot be ignored at higher concentrations of 2-naphthol, which reduces the adsorption of berberine hydrochloride. Because adsorption of 2-naphthol mainly takes place in the micropores and mesopores of TEPA, while that of Congo red predominantly occurs in the macropores, hence as shown in Fig. 4c, the adsorption of Congo red from its single-component solution is almost the same as that from the mixture solution.

Langmuir and Freundlich isotherm models are applied to correlate the adsorption isotherm data (Table 3). It is observed that the Freundlich model can describe the adsorption isotherms better than Langmuir model for the adsorption of 2-naphthol from the mixture solutions with berberine hydrochloride, while Langmuir model is better than Freundlich model for characterizing the adsorption from the mixture solution with Congo red, which further confirms the different effect of berberine hydrochloride and Congo red on the adsorption of 2-naphthol from the mixture solution. Additionally, it is observed that the Langmuir isotherm fits better for the adsorption of berberine hydrochloride from the mixture solution, which is quite different from the results from its single solution. These results might further confirm that the surface of TEPA covered by 2-naphthol is more similar to be an ideal surface than that from the single-component solutions. Similar to the adsorption from the single-component solution, the adsorption of

Congo red from the mixture solution can also be described by the Freundlich model.

The competitive adsorption between 2-naphthol, berberine hydrochloride, and Congo red on the TEPA adsorbent was also studied by exposing the TEPA sample to one of the adsorbates then measuring the adsorption isotherms of another adsorbate. After adsorbing berberine hydrochloride or Congo red (the initial concentration of berberine hydrochloride or Congo red was set to be 400 mg/L), the TEPA resins were washed with a small amount of water and further employed to adsorb 2-naphthol at different concentrations. As displayed in Fig. 5a, adsorption of 2-naphthol is reduced after the TEPA adsorbent is preloaded with berberine hydrochloride or Congo red, and the impact of berberine hydrochloride is more profound than that of Congo red. This is basically because both berberine hydrochloride and Congo red adsorb preferentially in the mesopores and macropores that are more accessible to these two adsorbates, which could partially block the entrance of the micropores and smaller mesopores (<1.5 nm). Because the molecular size of berberine hydrochloride (1.47 nm × 0.66 nm × 0.32 nm) is smaller than that of Congo red (2.29 nm × 0.82 nm × 0.60 nm), the blockage by the berberine hydrochloride is greater than Congo red, so the adsorption sites available for 2-naphthol are less, and the adsorption capacity reduction is greater when TEPA is preloaded with berberine hydrochloride. The isotherms were fitted by Langmuir and Freundlich isotherm models, and the equation constants are summarized in Table S. Neither of Langmuir nor Freundlich isotherm models can fit the adsorption of 2-naphthol after adsorption of berberine hydrochloride, but the Freundlich isotherm model can describe the adsorption of 2-naphthol after adsorption of Congo red.

After adsorption of 2-naphthol, the adsorption isotherms of berberine hydrochloride or Congo red on TEPA are shown in Fig. 5b and c, respectively. It can be seen that the adsorption of Congo red on TEPA after adsorption of 2-naphthol is the same as the adsorption from the single-component solution, suggesting different adsorption sites for these two adsorbates, and 2-naphthol is mainly adsorbed in the micropore and mesopores, while Congo red is adsorbed in the macropores. On the other hand, the adsorption isotherm of berberine hydrochloride after adsorption of 2-naphthol is similar to that obtained from the mixture solution (Fig. 4b). A similar explanation on the mixture adsorption can be applied here. The fitted results (Table 4) showed that both of Langmuir and Freundlich models are suitable for describing the adsorption data of berberine hydrochloride after adsorption of 2-naphthol.

3.4. Adsorption kinetics

Fig. 6 displays the adsorption kinetic curves of 2-naphthol, berberine hydrochloride, and Congo red on TEPA from the single-component solution at 298 K. It was observed that the adsorption

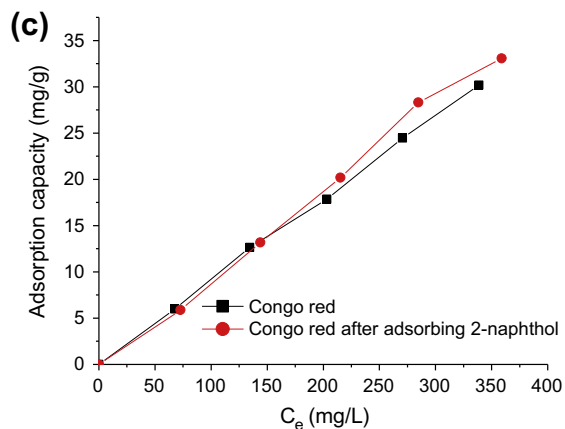
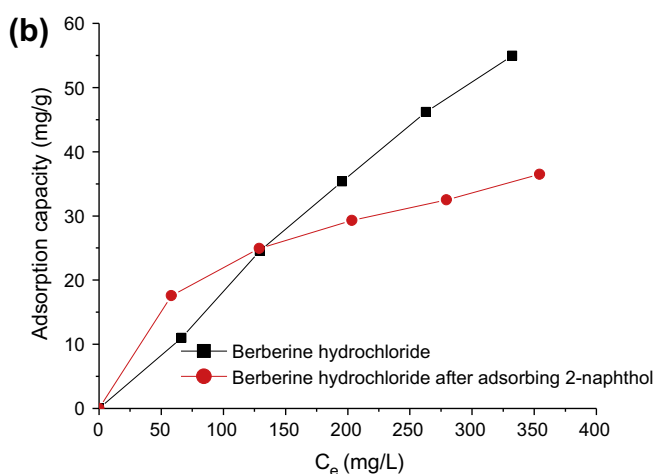
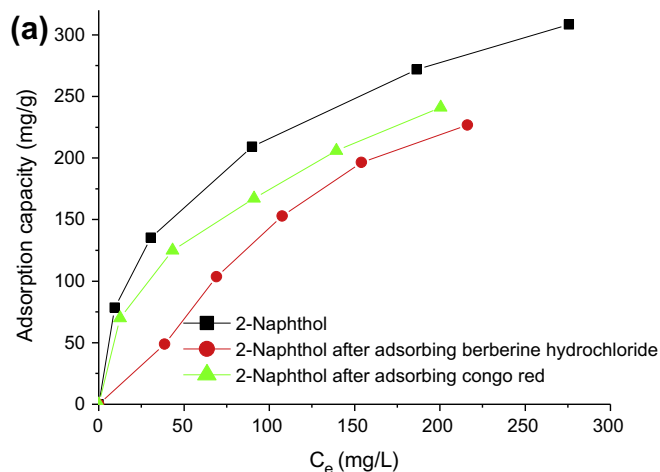


Fig. 5. Competitive adsorption isotherms of (a) 2-naphthol, (b) berberine hydrochloride, (c) Congo red after the TEPA preloaded with an adsorbate.

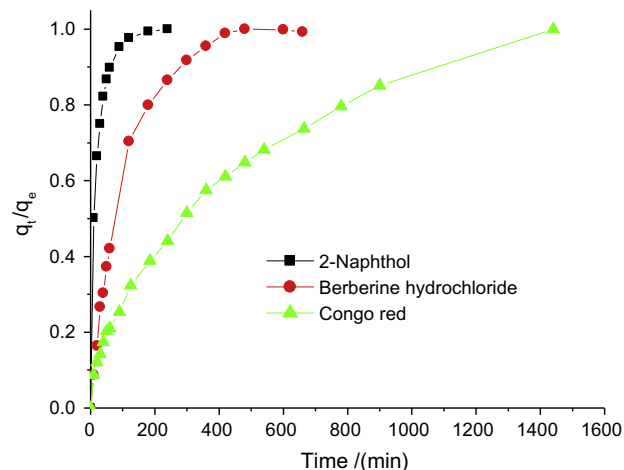


Fig. 6. Adsorption uptake curves of 2-naphthol, berberine hydrochloride, and Congo red on TEPA resin from aqueous solutions.

of 2-naphthol on TEPA is very fast in the first hour (reaches 90% of the equilibrium capacity) and arrives at the equilibrium within 180 min. With the increase in adsorbate molecular size, the time required for reaching adsorption equilibrium also increases. For berberine hydrochloride, the adsorption is much slower than that of 2-naphthol; only 40% of the equilibrium capacity is obtained in the first 1 h, and more than 480 min are required to reach the equilibrium. For Congo red, the adsorption does not reach equilibrium even after 24 h later. These observations imply that it is possible to achieve a good separation of 2-naphthol and berberine hydrochloride by exploring the difference of adsorption kinetics of these two molecules.

Typically, the Lagergren's rate equation (pseudo-first-order rate equation) and the pseudo-second-order equation proposed by Ho and McKay [35,36] are frequently employed for analyzing the adsorption kinetic data, and they can be represented as:

$$\text{Pseudo-first-order: } \ln(1 - F) = -k_1 t \quad (5)$$

$$\text{Pseudo-second-order: } \frac{t}{q_t} = \frac{1}{k_2 q_e^2} + \frac{1}{q_e} t \quad (6)$$

where k_1 and k_2 are the pseudo-first-order rate (1/min) and the pseudo-second-order rate constant (g/(mg min)), and F is the fractional attainment of the equilibrium as $F = q_t/q_e$.

The fitted parameters and the correlation coefficients R^2 for the pseudo-first-order and pseudo-second-order rate equation are summarized in Table 5. The pseudo-second-order rate equation is shown to be more appropriate for describing the kinetic data of berberine hydrochloride and 2-naphthol, while both equations cannot fit the kinetic data for the adsorption of Congo red very well. In addition, the initial adsorption rate v_0 , where $v_0 = k_2 q_e^2$ calculated in Table 5, indicates that these three adsorbates have an

Table 4

The fitted results for the sited adsorption of berberine hydrochloride or Congo red on TEPA after adsorbing 2-naphthol according to Langmuir and Freundlich isotherm models.

	Langmuir isotherm model			Freundlich isotherm model		
	q_m (mg/g)	K_L (L/mg)	R^2	K_F [(mg/g)(L/mg) ^{1/n}]	n	R^2
<i>Berberine hydrochloride</i>						
Single adsorbate solution	1316	1.367×10^{-4}	0.05984	0.1780	1.003	0.9917
After adsorbing 2-naphthol	45.81	9.595×10^{-3}	0.9902	3.561	2.527	0.9969
<i>Congo red</i>						
Single adsorbate solution	2326	3.896×10^{-5}	0.02492	9.119×10^{-2}	1.003	0.9982
After adsorbing 2-naphthol	/	/	0.5140	5.350×10^{-2}	0.9074	0.9964

Table 5
The fitted results for the kinetic data of 2-naphthol, berberine hydrochloride, and Congo red on TEPA according to the pseudo-first-order and pseudo-second-order rate equations.

	Pseudo-first-order		Pseudo-second-order			
	k_1 (1/min)	R^2	q_e (mg/g)	k_2	v_0 (mg/(g min))	R^2
2-Naphthol	3.171×10^{-2}	0.9319	108.9	8.499×10^{-4}	10.09	0.9998
Berberine hydrochloride	8.990×10^{-3}	0.9564	68.35	1.384×10^{-4}	0.6465	0.9943
Congo red	2.150×10^{-3}	0.9770	74.35	5.037×10^{-5}	0.2784	0.9633

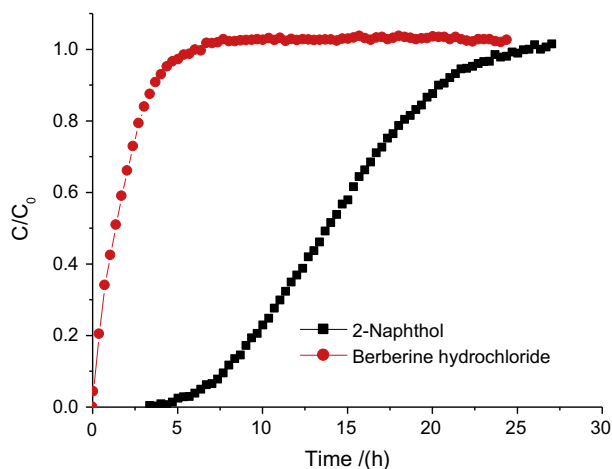


Fig. 7. Adsorption breakthrough curves of berberine hydrochloride and 2-naphthol from a TEPA column using a mixture solution.

order of v_0 (2-naphthol) $\gg v_0$ (berberine hydrochloride) $> v_0$ (Congo red), which agrees with the time required for reaching the adsorption equilibrium.

3.5. Dynamic separation of berberine hydrochloride from the mixture solution

Both adsorption equilibrium and kinetics results for these three adsorbates discussed above imply the possibility of removing 2-naphthol from berberine hydrochloride or 2-naphthol from Congo red using the TEPA adsorbent. In order to demonstrate the separation capability of TEPA as a specific polymeric adsorbent for removing small organic molecules from a mixture solution containing berberine hydrochloride and other smaller organic molecules, an adsorption column breakthrough experiment for dynamic adsorption and separation of 2-naphthol and berberine hydrochloride from a mixture sample was performed. The adsorption breakthrough curve of both components is plotted in Fig. 7.

Fig. 7 indicates that berberine hydrochloride is leaked out directly after starting the dynamic separation experiment, while 2-naphthol does not leak out until 6.4 h (at $C/C_0 = 0.05$), and the breakthrough point of 2-naphthol from the mixture solution is measured to be 107 BV. So, it is clear that TEPA can separate 2-naphthol and berberine hydrochloride as the effluent is in the range of 0–107 BV, and the purity of berberine hydrochloride before the breakthrough point of 2-naphthol increases from 66.7% (mass fraction, in the initial mixture sample) to 99.4% (in the effluent). Meanwhile, a desorption experiment demonstrates that a mixture solution containing 50% of ethanol and 1% of NaOH aqueous solution can completely regenerate the TEPA resin, and nearly 100% regeneration efficiency can be achieved, implying that TEPA could be an effective polymeric adsorbent for concentrating berberine hydrochloride from aqueous solutions by removing smaller organic molecules.

4. Conclusions

A hypercrosslinked PS resin TEPA was successfully synthesized from a chloromethylated PS by using the Friedel–Crafts and amination reactions. The TEPA adsorbent is characterized with different analytical techniques for its physical and chemical properties. It was observed that the pore structure the TEPA adsorbent consists of microporous and mesoporous structure in addition to a small portion of macropores. The TEPA adsorbent adsorbs 2-naphthol from aqueous solutions very efficiently due to the micropore filling mechanism. With the increase in the molecular size of the adsorbate, the adsorption on TEPA was much weakened; only about 15% of berberine hydrochloride and 13% of Congo red are adsorbed on the TEPA adsorbent from aqueous solutions, exhibiting a strong molecular sieving effect of the TEPA adsorbent. The adsorption kinetic data indicate that the adsorption of 2-naphthol on the TEPA adsorbent is fast, adsorption of berberine hydrochloride is much slower, and that of Congo red is the slowest. The separation capability of the TEPA adsorbent for concentrating berberine hydrochloride was well demonstrated in an adsorption column breakthrough experiment; the purity of berberine hydrochloride increases from 66.7% to 99.4%. The TEPA adsorbent synthesized in this work is a very promising specific polymeric adsorbent for concentrating and purifying berberine hydrochloride and other similar alkaloids from the herbal plant extracts.

Acknowledgments

This work was partially supported by the National Natural Science Foundation of China (Nos. 21176218, 21174163), Zhejiang Key Innovation Team of Green Pharmaceutical Technology (Project No.: 2010R50043), and the Hengyi Fund of Zhejiang University.

Appendix A. Supplementary material

Supplementary data associated with this article can be found, in the online version, at <http://dx.doi.org/10.1016/j.jcis.2013.03.011>.

References

- [1] H. Li, Y.Z. Li, Z.P. Li, X.Y. Peng, Y.N. Li, G. Li, X.Z. Tan, G.X. Chen, Appl. Surf. Sci. 258 (2012) 4314–4321.
- [2] A.M. Zhu, J.H. Chen, Q.L. Liu, Y.L. Jiang, J. Appl. Polym. Sci. 120 (2011) 2374–2380.
- [3] G.Q. Xiao, S.Q. Gao, X.L. Xie, M.C. Xu, Polym. Adv. Technol. 20 (2009) 1157–1162.
- [4] X.J. Li, Y.J. Fu, M. Luo, W. Wang, L. Zhang, C.J. Zhao, Y.G. Zu, J. Pharm. Biomed. Anal. 61 (2012) 199–206.
- [5] G.P. Pi, P. Ren, J.M. Yu, R.F. Shi, Z. Yuan, C.H. Wang, J. Chromatogr. A 1192 (2008) 17–24.
- [6] D. Falkenhagen, W. Strobl, G. Vogt, A. Schreffl, I. Linsberger, F.J. Gerner, M. Schoenhofen, Int. Soc. Artificial Organs 23 (1999) 81–86.
- [7] B.J. Pan, W.M. Zhang, B.C. Pan, H. Qiu, Q.R. Zhang, Q.X. Zhang, S.R. Zheng, Environ. Sci. Technol. 42 (2008) 7411–7416.
- [8] W.M. Zhang, C.H. Hong, B.C. Pan, Z.W. Xu, Q.J. Zhang, L. Lv, J. Hazard. Mater. 158 (2008) 293–299.
- [9] J.H. Huang, G. Wang, K.L. Huang, Chem. Eng. J. 168 (2011) 715–721.
- [10] Z.Y. Xu, Q.X. Zhang, J.L. C, L.S. Wang, G.K. Anderson, Chemosphere 38 (1999) 2003–2011.
- [11] J.H. Huang, X.Y. Jin, J.L. Mao, B. Yuan, R.J. Deng, S.G. Deng, J. Hazard. Mater. 217–218 (2012) 406–415.

- [12] J.H. Huang, J. Appl. Polym. Sci. 121 (2011) 3717–3723.
- [13] J.H. Huang, X.L. Wang, X.M. Wang, K.L. Huang, Ind. Eng. Chem. Res. 50 (2011) 2891–2897.
- [14] M.P. Tsyurupa, V.A. Davankov, React. Funct. Polym. 66 (2006) 768–779.
- [15] V. Davankov, M. Tsyurupa, J. Chromatogr. A 1087 (2005) 3–12.
- [16] V. Davankov, M. Tsyurupa, M. Ilyin, L. Pavlova, J. Chromatogr. A 965 (2002) 65–73.
- [17] V.A. Davankov, M.P. Tsyurupa, N.N. Alexienko, J. Chromatogr. A 1100 (2005) 32–39.
- [18] A.M. Li, Q.X. Zhang, G.C. Zhang, J.L. Chen, Z.H. Fei, F.Q. Liu, Chemosphere 47 (2002) 981–989.
- [19] M.P. Tsyurupa, V.A. Davankov, React. Funct. Polym. 53 (2002) 193–203.
- [20] C.F. Chang, C.Y. Chang, K.E. Hsu, S.C. Lee, W. Holl, J. Hazard. Mater. 155 (2008) 295–304.
- [21] X.H. Yuan, X.H. Li, E.B. Zhu, J. Hu, W.C. Sheng, S.S. Cao, Carbohydr. Polym. 74 (2008) 468–473.
- [22] C.L. He, J.H. Huang, C. Yan, J.B. Liu, L.B. Deng, K.L. Huang, J. Hazard. Mater. 180 (2010) 634–639.
- [23] C.G. Oh, J.H. Ahn, S.K. Ihm, React. Funct. Polym. 57 (2003) 103–111.
- [24] C.P. Wu, C.H. Zhou, F.X. Li, Experiments of Polymeric Chemistry, Anhui Science and Technology Press, Hefei, 1987.
- [25] B.L. He, W.Q. Huang, Ion Exchange and Adsorption Resin, Shanghai Science and Technology Education Press, Shanghai, 1995.
- [26] J.H. Ahn, J.E. Jang, C.G. Oh, S.K. Ihm, J. Cortez, D.C. Sherrington, Macromolecules 39 (2005) 627–632.
- [27] F.S. Macintyre, D.C. Sherrington, Macromolecules 37 (2004) 7628–7636.
- [28] J.H. Huang, B. Yuan, X.F. Wu, S.G. Deng, J. Colloid Interface Sci. 380 (2012) 166–172.
- [29] B.P. Bering, M.M. Dubinin, V.V. Serpinsky, J. Colloid Interface Sci. 21 (1966) 378–393.
- [30] J. Skopp, J. Chem. Educ. 86 (2009) 1341.
- [31] Y.J. Fu, Y.G. Zu, W. Liu, C.L. Hou, L.Y. Chen, S.M. Li, X.G. Shi, M.H. Tong, J. Chromatogr. A 1139 (2007) 206–213.
- [32] S. Battu, M. Repka, S. Maddineni, A. Chittiboyina, M. Avery, S. Majumdar, AAPS PharmSciTech 11 (2010) 1466–1475.
- [33] M.P. Moyle, M. Tyner, Ind. Eng. Chem. 45 (1953) 1794–1797.
- [34] R.S. Juang, J.Y. Shiau, J. Hazard. Mater. 70 (1999) 171–183.
- [35] H. Qiu, L. Lv, B.C. Pan, Q.J. Zhang, W.M. Zhang, Q.X. Zhang, J. Zhejiang Univ. – Sci. A 10 (2009) 716–724.
- [36] Y.S. Ho, G. McKay, Chem. Eng. J. 70 (1998) 115–124.